
Article:
Meng, X., Pullen, A., Guo, X. et al. (2 more authors) (2023) Applications of 3D scanning and digital image correlation in structural experiments. ce/papers, 6 (3-4). pp. 1674-1679. ISSN 2509-7075

https://doi.org/10.1002/cepa.2543

Applications of 3D scanning and digital image correlation in structural experiments

Xin Meng[1] | Andy Pullen[1] | Xi Guo[1] | Xiang Yun[2] | Leroy Gardner[1]

1 Introduction

Physical experiments are an essential element in structural research. They provide evidence to structural researchers for explaining a new phenomenon, verifying an existing theory, validating a numerical model and ultimately developing appropriate design guidance for the industry. The measurements of geometric properties and structural responses in an experiment have long relied on conventional equipment such as callipers, strain gauges and transducers, which, although generally serving their purposes, can be tedious in terms of repeated measurements or installation and provide limited information only at discrete locations of interest. In recent years, two novel data acquisition techniques – 3D scanning and digital image correlation (DIC), have emerged and are gaining increasing popularity in experimental structural research. In this paper, the basics and workflows of 3D scanning and DIC are described, and their applications in structural experiments, with a particular focus on metallic materials and structures, are subsequently presented along with examples. The aim of the present research is to demonstrate the benefits of 3D scanning and DIC, and to provide guidance on how to use them effectively in structural experiments.

2 3D scanning

In this section, an introduction to 3D scanning is firstly presented, followed by a brief review of its existing applications in structural engineering and other disciplines. Finally, the typical workflow of 3D scanning is described.

2.1 Introduction

3D scanning is the process of acquiring 3D surface geometric data of an object. A variety of techniques is available for 3D scanning, which can be broadly categorised as contact and non-contact techniques, as shown in Figure 1. Contact methods generally involve probing through contact, while non-contact techniques can be further categorised as active and passive techniques, depending on whether active emission of a certain type of radiation or light is required. Among these 3D scanning techniques, laser scanning and structured light scanning are currently the most widely used ones for structural engineering research purposes. Laser scanning is capable of obtaining full and detailed information of the examined surface geometry with excellent efficiency and accuracy by detecting the deflection of actively projected laser beams, while structured light scanning is a similar technique but based on a pattern of white or blue light projected onto the examined object.

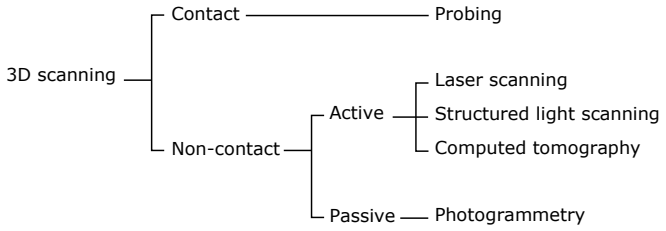

Figure 1 Categorisation of 3D scanning techniques

3D scanning technology has gained broad applications across various disciplines, such as reverse engineering, surveying and archaeology. The use of 3D scanning in civil engineering has also been on the rise in recent years. Terrestrial laser scanners have been widely employed in structural monitoring and health assessment [1]. The creation of building information models (BIM), which has long been a time-consuming and error-prone process, is being revolutionised by the use of 3D scanning for data acquisition [2]. 3D scanning has also been increasingly utilised in structural testing, primarily for the determination of dimensional properties and characterisation of initial geometric imperfections. With the growing research interest in metal additive manufacturing, particularly wire arc additive manufacturing (WAAM), 3D scanning becomes crucial for capturing the unique geometric features inherent to the printing process [3]. Further discussions on its use in structural experiments are provided in Section 3.

2.2 Workflow

In this subsection, the workflow of 3D scanning is demonstrated by examining a generic structural steel I-section specimen. A Faro Design ScanArm laser scanner, which is capable of capturing up to 500,000 points per second with an accuracy of 0.1 mm and point resolution of 40–75 μm, was employed, as shown in Figure 2. The laser scanner was set up in a controlled environment – in particular, an air conditioner was employed to minimise the change in temperature when laser scanning was performed. The test specimen was placed on a working platform, which was carefully stabilised to prevent any movement of the examined object during the scanning operation.

Figure 2 Setup for laser scanning

Prior to scanning, the laser scanner was calibrated and compensated following the procedure set out by the manufacturer. In case of occlusion or limitations due to the working range/volume of the adopted scanner, multiple scans are required to obtain the full surface geometry of the examined object. To demonstrate this process, the outer surface geometry of the examined I-section specimen was captured in two scans, with magnets attached onto the sample as features to facilitate subsequent data registrations.

The data processing procedure is illustrated in Figure 3. The raw point clouds were initially processed to remove the unwanted data. Data registration, a process where the multiple point clouds are transformed from their respective local coordinate systems into a global coordinate system with errors being minimised, was performed. In the example case, a coarse (manual) registration was initially performed to estimate the rigid motion required between the two point clouds. A fine registration was subsequently performed using the global registration command in Geomagic Wrap [4], where the transformation of the scans was refined in an iterative manner by minimising the distances between the correspondence and eventually converged to the most accurate solution.

Figure 3 Processing of 3D scanned data of a structural steel I-section specimen

The accuracy of the point cloud registration was assessed

based on the distribution of deviations between the overlapping point clouds. In this case, as shown in Figure 3, the deviations were generally below 0.01 mm, with a mean deviation equal to 0.002 mm, which was deemed satisfactory. The artificial features in the point cloud data (i.e. the scans of the magnets) were manually removed, and finally the point cloud was converted to a polygon object with mesh repairments applied where necessary.

3 Applications of 3D scanned data with examples

In this section, example applications of 3D scanned data in experimental studies on metallic structures, including the determination of dimensional properties and characterisation of geometric imperfections, are presented.

3.1 Dimensional properties

The key dimensional parameters of test specimens can be directly extracted from the 3D scanned data; this is particularly useful when dealing with complex specimen geometry, such as wire arc additively manufactured (WAAM) specimens which exhibit inherent surface undulations.

In [3], the 3D laser scanning technique was employed to examine WAAM steel square hollow section (SHS) specimens. The raw point clouds were initially gridded with a spacing of 0.2 mm, and key cross-section dimensions, including the height H, breadth B, wall thickness and cross-sectional area of the examined WAAM SHS specimens were obtained by analysing contours of the scans at 0.2 mm intervals along the longitudinal direction, as illustrated in Figure 4. Typical distributions of the outer dimensions along the length derived from the scanned data are plotted in Figure 5.

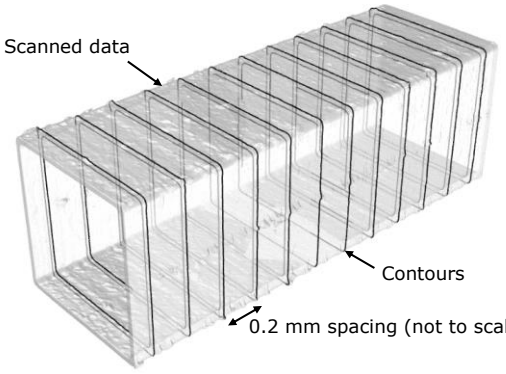

Figure 4 Determination of cross-section dimensions of WAAM SHS based on a series of contours from 3D scanned data

Figure 5 Typical distributions of cross-section dimensions along length of WAAM SHS from 3D scanned data

3.2 Geometric imperfections

With the ability to efficiently capture the full surface geometry, 3D scanning naturally enables researchers to gain a deeper insight into the distribution of geometric imperfections in structural elements. A consistent approach to characterising the local geometric imperfections in flat plates from 3D scanned data was proposed in [5]. Three types of local geometric imperfections – cross-section imperfections (out-of-straightness of a nominally straight edge at the cross-sectional level), plate imperfections (out-of-flatness of a plate element) and longitudinal imperfections (out-of-straightness along a series of longitudinal lines on a plate element), were proposed, and a typical distribution of local geometric imperfections in a plate element, derived from the 3D scanned data, is shown in Figure 6(a). In [6], a similar definition to longitudinal imperfections was adopted to characterise the local geometric imperfections in cylindrical and corrugated shells from the 3D scanned data, as exemplified in Figure 6(b). Furthermore, global geometric imperfections in a structural member can also be determined from the 3D scanned data by examining the centroids of contours along the length (similar to Figure 4), as successfully carried out in [7].

a) Plate imperfections in a flat plate (dimensions in mm)

b) Longitudinal imperfections in a corrugated shell

Figure 6 Typical distributions of local geometric imperfections from 3D scanned data

4 Digital image correlation (DIC)

The basic principles of digital image correlation (DIC) are initially introduced in this section. A generic stub column test featuring a stereo DIC system is subsequently described to demonstrate the typical workflow of DIC.

4.1 Introduction

Digital Image Correlation (DIC) is a non-contact technique for monitoring the motion and deformation of an object. By tracking and correlating patterns in digital images, the coordinate fields on the surface of a test specimen can be constructed, based on which the full-field history of the quantities of interest, such as displacements, strains and velocities, can then be derived [8]. This approach was proposed in 1975 for generating terrain data from overlapping aerial photographs using optical-density scans of the original film negatives [9]. The advance of DIC algorithms and the reducing costs of the hardware have facilitated the rapid adoption and widespread use of DIC in recent years.

A stereo DIC system typically consists of a matched pair of high-resolution monochrome digital cameras, fitted with matched prime (fixed focal-length) lenses and attached to a stable mounting, such that their relative positions and orientations remain unchanged throughout the duration of an experiment. A controller may also be required, primarily for precisely timing and synchronising image capture, as well as a PC. This hardware may be controlled by commercial software, which also carries out the calibration and DIC data processing, though it is possible to utilise independent hardware and import the acquired images later into appropriate open-source software or self-developed programmes for data analysis. Stereo DIC is generally favoured if available, although 2D DIC using one single camera is also possible when the region of interest is planar with only in-plane behaviour during the experiment. DIC can also be implemented based on microscopic images or using high-speed cameras, which further increases the versatility of this technology.

Thus far, DIC has been widely used in experimental studies from various disciplines, including material science, automotive and aerospace engineering, geology and biomechanics. The use of DIC in civil engineering applications has also been growing rapidly. In structural health monitoring, DIC has been successfully used for, e.g. crack detection [10] and movement tracking [11], without interfering with the structural functionalities. Structural testing also has started to embrace this novel technique; further discussions on the effective use of DIC in the testing of metallic materials and structures are provided in Section 5.

4.2 Workflow

To demonstrate the workflow of DIC, a compression test on a cold-formed steel square hollow section (SHS) stub column is described in this subsection, with stereo DIC employed to monitor the local buckling behaviour of a flat constituent plate. The test setup is shown in Figure 7. The SHS specimen was placed between a pair of hardened high strength steel end plates, and a ball seating was employed at the top to accommodate any out-of-squareness of the specimen ends. A two-camera stereo DIC system from LaVision was employed. The DIC cameras were set up at a stereo angle of approximately 34° to facilitate depth measurements. Speckle patterns were applied to the monitored surface using anti-reflective paints to provide trackable features for DIC. The speckle size was chosen such that the average speckle size in the DIC camera is 3 to 5 pixels to avoid aliasing [12]. Additional LED lights were used to improve the intensity and uniformity of illumination over the region of interest.

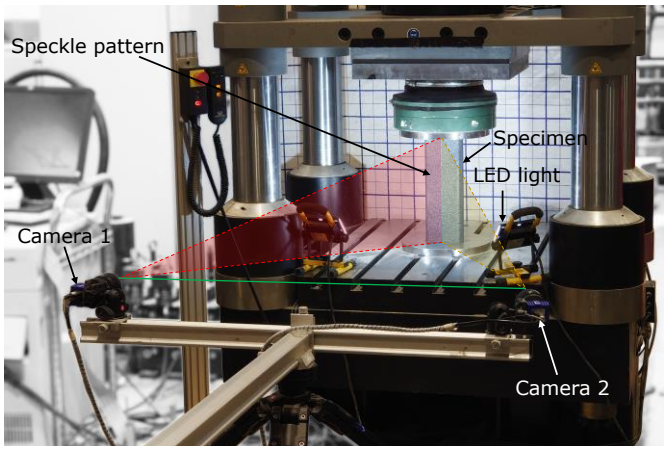

Figure 7 Setup of stereo DIC for a stub column test

Upon setting up, the stereo DIC system was calibrated, using standard calibration plates (Figure 8), to determine both the intrinsic camera parameters (e.g. image scale, focal length and lens distortions) and the extrinsic parameters (e.g. stereo angle, distance between cameras and distance from cameras to object) [8]. A trial DIC test was then carried out to verify the quality of speckle patterns and calibration.

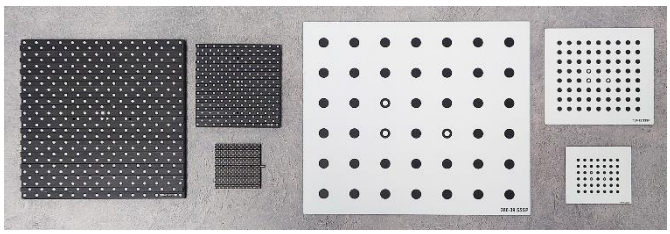

Figure 8 Typical DIC calibration plates: 3D (left) and 2D plates (right)

Finally, the compression test was performed with the DIC images taken at a frequency of 0.5 Hz and recorded using Davis 10 [13] along with the applied load and machine displacement. The processing of DIC data was also performed using Davis 10 [13].

5 Applications of DIC data with examples

There have been a number of studies attempting to use DIC in the testing of metallic structures, ranging from material tests up to large-scale structural system tests. In this section, example applications are presented to demonstrate the capability and potential of DIC in structural experiments.

5.1 Material tests

Material tests are commonly performed to determine key mechanical properties of the examined material. As

opposed to strain gauges and extensometers, DIC is capable of providing the full-field strain responses of the test specimens. An example tensile test on a coupon specimen extracted from a hot-rolled S355 steel profile is presented herein. Two stereo DIC systems were employed to monitor the strain fields on both sides of the coupon within the parallel length. Typical longitudinal strain fields obtained from the DIC data are displayed on the engineering stress-strain curve in Figure 9. Phenomena such as the initiation of yielding, Lüders banding and necking, which cannot be easily captured using conventional instrumentation, are now clearly visualised by the DIC results.

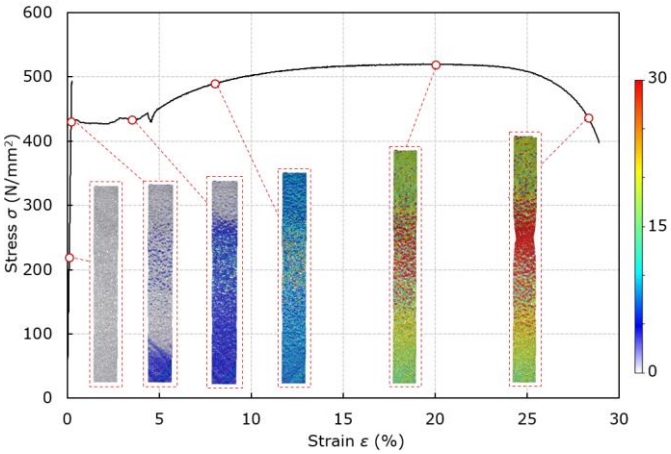

Figure 9 Typical longitudinal strain fields (in %) from DIC for a tensile coupon test

In addition, DIC has also been utilised for tensile coupon tests involving non-uniform strain responses (e.g. for WAAM materials and welded coupons [14]), residual stress measurements [15], fatigue tests [16] and fracture tests [17].

5.2 Structural element tests

A number of experimental studies on structural elements has featured DIC to gain a deeper insight into their structural responses. In [5] and [18], stereo DIC was adopted to examine the local buckling behaviour of high strength steel tubular section specimens under axial compression and combined loading. Typical longitudinal strain fields obtained from the DIC data, as shown in Figure 10, quantitatively reveal the local buckling shapes under different loading scenarios. DIC has also been employed in member buckling tests to monitor the global buckling behaviour, such as [7].

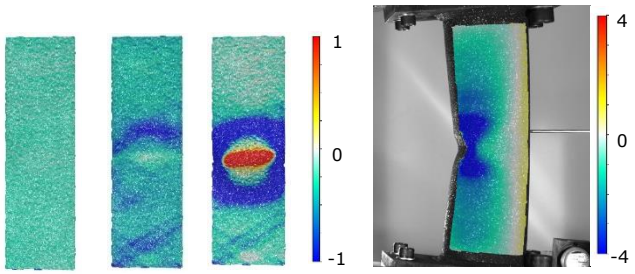

Figure 10 Typical longitudinal strain fields (in %) from DIC for a stub column test (left) and a combined loading test (right)

In connection tests, DIC enables a more in-depth study into the complex failure mechanisms of the tested connections. An experimental programme on WAAM steel bolted single-shear connections was conducted featuring DIC and reported in [19]. Two stereo DIC systems were set up on both sides of the examined single-shear connection specimens, as shown in Figure 11(a), to monitor the strain and displacement fields on the constituent plates. Typical longitudinal strain fields over the WAAM plate obtained from the DIC data are shown in Figure 11(b), where a butterfly-shaped strain distribution was observed at the ultimate load stage, indicating a localised tearing failure mode.

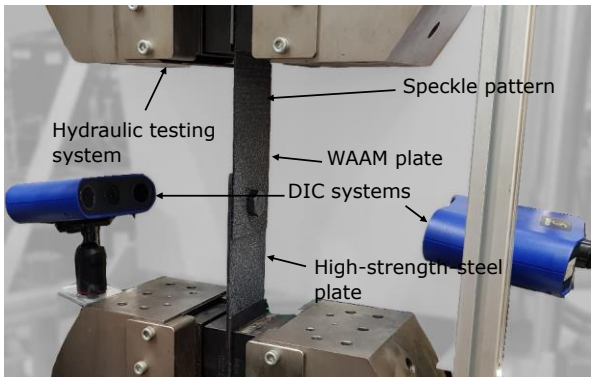

a) Setup of two stereo DIC systems for single-shear connection tests

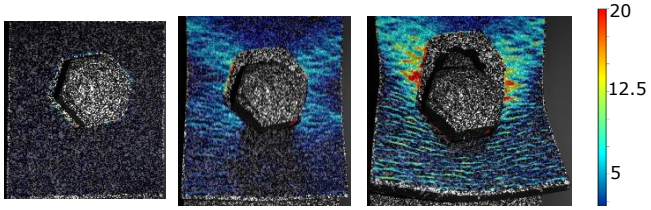

b) Longitudinal strain fields from DIC (in %)

Figure 11 Application of DIC in single-shear connection tests

5.3 Structural system tests

In large-scale structural system tests, DIC is also capable of providing accurate, reliable and detailed information concerning the fields of displacement and strain within either regions of particular interest or the whole tested system. A series of experiments on high strength steel frames was conducted in [20], in which two stereo DIC systems were employed to measure both full-field displacements of the entire frame specimen, and the localised strain development within the region where the first plastic hinge formed. The DIC results at the maximum applied load from a typical frame test are shown in Figure 12.

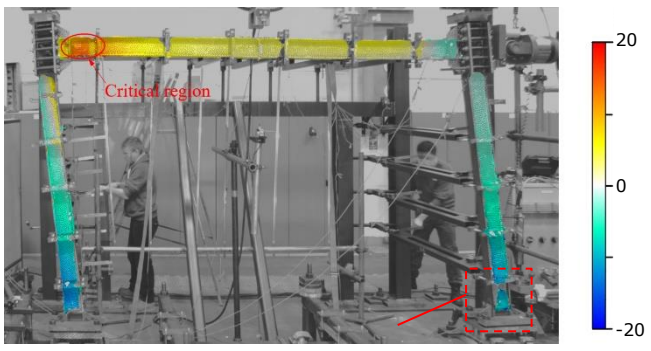

Figure 12 Out-of-plane displacement field (in mm) for entire frame and localised longitudinal strain field (in %) at column base from DIC

These comprehensive DIC measurements provided additional information that enabled a better understanding of the structural behaviour of the examined high strength steel frames.

6 Conclusions

3D scanning is addressed in the first part of the paper. The basics of 3D scanning is firstly described, followed by a brief review of its applications in civil engineering and other disciplines. By examining a generic structural steel I-section sample, the typical workflow of 3D scanning is presented. The use of 3D scanning in experimental studies on metallic structures, predominantly for the determination of specimen geometries and the characterisation of geometric imperfections, is discussed with examples provided.

The second part of the paper is focussed on digital image correlation (DIC). A brief introduction to DIC, covering the basic principles, components of typical DIC systems and current applications, is initially provided. The workflow for setting up a stereo DIC system is subsequently described through an example stub column test. DIC is gaining increasing application in material tests, local and global buckling tests, connection tests and structural system tests, examples of which are presented and discussed.

The presented study clearly demonstrates the benefits and potential of 3D scanning and DIC in the testing of metallic materials and structures, and provides guidance on the effective use of these techniques in structural experiments.

References

[1] Mukupa, W.; Roberts, G.W.; Hancock, C.M.; Al-Manasir, K. (2017) *A review of the use of terrestrial laser scanning application for change detection and deformation monitoring of structures*. Survey Review 49, 353, pp. 99–116.

[2] Li, D.; Liu, J.; Feng, L.; Yang, Z.; Qi, H.; Chen, Y.F. (2021) *Automatic modeling of prefabricated components with laser-scanned data for virtual trial assembly*. Computer-Aided Civil and Infrastructure Engineering 36, 4, pp. 453–471.

[3] Meng, X.; Weber, B.; Gardner, L. (2023) *Optimisation and testing of wire arc additively manufactured steel stub columns.* Thin-Walled Structures (submitted).

[4] 3D Systems (2017) Geomagic Wrap 2017 [Software].

[5] Meng, X.; Gardner, L. (2020) *Testing of hot-finished high strength steel SHS and RHS under combined compression and bending.* Thin-Walled Structures 148, 106262.

[6] Zhang, R.; Gardner, L.; Amraei, M.; Buchanan, C.; Piili, H. (2023) *Testing and Analysis of Additively Manufactured Stainless Steel Corrugated Cylindrical Shells in Compression*. Journal of Engineering Mechanics 149, 4, 04023013.

[7] Huang, C.; Meng, X.; Buchanan, C.; Gardner, L. (2022) *Flexural Buckling of Wire Arc Additively Manufactured Tubular Columns*. Journal of Structural Engineering 148, 9, 04022139.

[8] Jones, E.M.C.; Iadicola, M.A. (2018) *A Good Practices Guide for Digital Image Correlation*. International Digital Image Correlation Society.

[9] Keating, T.J.; Wolf, P.R.; Scarpace, F.L. (1975) *An Improved Method of Digital Image Correlation*. Photogrammetric Engineering & Remote Sensing 41, 8, pp. 993-1002.

[10] McCormick, N.; Lord, J. (2012) *Digital image correlation for structural measurements*. Proceedings of the Institution of Civil Engineers-Civil Engineering 165, 4, pp. 185-190.

[11] Dhanasekar, M.; Prasad, P.; Dorji, J.; Zahra, T. (2019) *Serviceability assessment of masonry arch bridges using digital image correlation*. Journal of Bridge Engineering 24, 2, 04018120.

[12] Reu, P. (2014) *All about Speckles: Aliasing*. Experimental Techniques 38, pp. 1–3.

[13] LaVision GmbH (2019) DaVis 10. [Software].

[14] Yan, R.; El Bamby, H.; Veljkovic, M.; Xin, H.; Yang, F. (2021) *A method for identifying the boundary of regions in welded coupon specimens using digital image correlation*. Materials and Design 210, 110073.

[15] Nelson, D.V.; Makino, A.; Schmidt, T. (2006) *Residual stress determination using hole drilling and 3D image correlation*. Experimental Mechanics 46, 1, pp. 31–38.

[16] Rupil, J.; Roux, S.; Hild, F.; Vincent, L. (2011) *Fatigue microcrack detection with digital image correlation*. Journal of Strain Analysis for Engineering Design 46, 6, pp. 492–509.

[17] Paredes, M.; Grolleau, V.; Wierzbicki, T. (2020) *On ductile fracture of 316L stainless steels at room and cryogenic temperature level: An engineering approach to determine material parameters*. Materialia 10, 100624.

[18] Meng, X.; Gardner, L. (2020) *Cross-sectional behaviour of cold-formed high strength steel circular hollow sections.* Thin-Walled Structures 156, 106822.

[19] Guo, X.; Kyvelou, P.; Ye, J.; Teh, L.H.; Gardner, L. (2022) *Experimental investigation of wire arc additively manufactured steel single-lap shear bolted connections*. Thin-Walled Structures 181, 110029.

[20] Yun, X.; Zhu, Y.; Wang, Z.; Gardner, L. (2022) *Benchmark tests on high strength steel frames*. Engineering Structures 258, 114108.